American Journal of Materials Science 2024, 14(1): 1-11
DOI: 10.5923/j.materials.20241401.01

Optical and Electrical Characterization of SnO_2:Ga and Sb-co-doped SnO_2:Ga Thin Films Prepared by Sol-Gel Dip-Coating Method

Sally Kemuma Gichana*, David M. Mulati, Timonah N. Soitah

Department of Physics: Jomo Kenyatta University of Agriculture and Technology (JKUAT), Nairobi, Kenya

Abstract P-type Gallium doped tin oxide and Antimony co-doped Gallium-tin oxide thin films have been prepared on blue plus microscope glass substrates using the sol-gel dip-coating method. In this paper, Optical and electrical properties of the prepared thin films are presented. The obtained transmittance spectrum of the undoped (pure) SnO_2 thin film is transparent with an average transmittance ranging between (61.1-81.1) % at a wavelength range of 400 nm to 900 nm respectively. The SnO_2:Ga films indicate an average transmittance of about (50.4-72.6) % at a wavelength range of between 400 nm to 900 nm respectively. The Sb-co-doped SnO_2:Ga thin films indicates a variation in the average transmittance of about (53.6-78.1) % at a wavelength range of 400 nm to 900 nm respectively. A reduction in the average transmittance with increase in doping levels is observed for all the Ga doped and Sb-co-doped thin films. Undoped (pure) SnO_2 thin film has a direct bandgap value of 3.89 eV while SnO_2:Ga thin films band gap values of between 4.07 eV to 4.15 eV was measured. The Sb-co-doped SnO_2:Ga thin films has band gap values of between 4.10 eV to 4.16 eV. Highest band gap value of 4.15 eV was obtained for the SnO_2:Ga thin film and 4.16 eV for Sb-co-doped SnO_2:Ga thin film. Optical band gap widening and then narrowing were observed for all the Ga doped and Sb-co-doped thin films. Conductivity types of the thin films indicate an n-type charge for the undoped SnO_2 thin film. All SnO_2:Ga thin films are p-type conductive. Low co-doped levels of Sb-co-doped SnO_2:Ga thin films are p-type conductive while higher level co-doping of Sb shifted the thin films to n-type conductive. I-V characteristics demonstrate an ohmic behaviour for all the films as the concentrations of Ga and Sb increased. The Sb-co-doped SnO_2:Ga thin films shows improved I-V characteristics.

Keywords P-type, Thin Films, Sol-Gel, Optical properties and Electrical properties

1. Introduction

The transparent conductive oxides (TCOs) are a special class of materials which exhibit appreciable level of electrical conductivity, high optical transparency in the visible range and high infrared reflectivity [1]. Due to the uniqueness of the properties of these materials, many advances in technology like the touch screen displays, solid-state sensors, organic light emitting diodes (OLEDs), liquid crystal displays and photovoltaic cells largely rely on their applications [2], [3]. However, compared to the n-type conductive TCOs, suitable p-type TCOs have not been well established [4], [5], [6]. The difficulty in achieving a variety of p-type TCOs comes about from the unique electronic configuration of the oxide materials. For n-type TCOs, Conduction Band Minimum (CBM) which is the transport path for electrons is mainly composed of spatially spread and delocalized orbitals. This facilitates low electron effective mass hence high electron mobility. On the contrary for p-type TCOs, the Valence Band Maximum (VBM) which is the transport path for holes is localized and anisotropic in nature. This results in a large hole effective mass thus making hole mobility low [7], [8]. This difficulty has led to an obstacle in forming p-n junctions for various optoelectronic applications [9]. Following the chemical design principle of the cations existing in oxide materials, a series of p-type TCOs have been discovered. Such TCOs include the copper-bearing oxides ($CuMO_2$, M=Al, Ga, In), binary copper oxides (CuO and Cu_2O) and zinc spinel oxides. Among these, a highly transparent p-type TCO consisting of Copper Aluminium oxide ($CuAlO_2$) have been developed. However, the films remain in question since the magnitude of its resistivity is greater as compared to that of n-type indium tin oxide [10], [11]. Zinc is also another p-type TCO especially when doped with or deposited under certain conditions. Due to the self-compensation effect, there still exists difficulty in manufacturing the TCO thereby decaying rapidly for any use [12].

Many transparent electronic devices especially the solar

* Corresponding author:
sallygichana22@gmail.com (Sally Kemuma Gichana)
Received: Feb. 9, 2024; Accepted: Feb. 26, 2024; Published: Mar. 9, 2024
Published online at http://journal.sapub.org/materials

cells which is the current world's clean energy focus has been affected. This is because of the current p-type TCO unsatisfactory performance. As a result, many industries have substituted it with semi-crystalline metallic organic materials which have otherwise affected the stability of the device and registering low efficiency as well. If there would be suitable p-type TCOs, transparent p-n junctions could be fabricated for various applications in the transparent electronic industry [9], [13], [14].

Tin (IV) oxide is one such TCO highlighted to various applications in optoelectronic industry and green energy devices due to its unique performance. [3], [15], [16]. SnO_2 is an n-type semiconductor with a direct band gap of 3.6 eV to 4.0 eV. It is characterized with a rutile structure (a=b= 4.738 Å, c=3.187 Å) [17], [18]. It has been widely used in various optoelectronic applications like gas sensors [19], solar cells [20], LEDs [21], [22], transistors [22] and photo detectors [23]. Various studies have shown much interest in the fabrication of varieties of p-type tin-based films especially using group (III) elements of the periodic table like Al and Ga. They are anticipated as a good p-type source due to their unique different structures and sizes [24], [25] i.e the radius of Ga (0.062 nm) is lesser than that of Sn (0.069 nm) [7], [10]. This enhances the solubility of Ga ions into the tin site as a result of the induced photo catalytic activity and photo-induced charge separation [25]-[31]. However, the main challenge for SnO_2 thin films in realization of a p-type charge is having high resistivity due to low intrinsic carrier density and mobility. Therefore, co-doping with Sb is anticipated to produce highly stable thermal-chemically resultant material. This is because Sb is compatible with SnO_2 especially in a certain level of doping where the Sb^{3+} acts as acceptor as compared to donors [32], [33], [34].

Transparent Ga-doped SnO_2 p-type conductive thin films have been previously been prepared on quartz glass substrates by DC and RF magnetron sputtering technique. Both groups demonstrated that the prepared films exhibited a visible transmittance above 80.0%. [30], [35]. P-type Ga-doped SnO_2 thin films have also been directly prepared with no post-deposition oxygen annealing and reported improved electrical properties [30].

A variety of deposition techniques have been employed to prepare tin-based thin films both physical methods and chemical-based methods. Such methods include; DC and RF magnetron sputtering [35], spray pyrolysis technique [36], chemical vapor deposition sputtering [37], thermal evaporation [38], pulsed laser deposition [39] and the sol-gel method [40]. The sol-gel method has demonstrated a number of advantages over the other methods of coatings and deposition such as, cost-effective, environmental friendly, easy to control the underlying materials and doping concentrations, it requires low temperature for film densification and results to the formation of a homogenous structure. [40], [41].

In this work, transparent p-type conductive thin film of tin with Gallium doping and Sb-co-doping using the sol-gel dip-coating method are presented and their optical and electrical properties suitable for transparent electronic applications are shown.

2. Experimental

2.1. Materials

Tin (IV) chloride of trace metal basis (99.95% purity) Sigma Aldrich, Gallium (III) chloride, ultra dry, 99.999% purity (metal basis) Sigma Aldrich, Ethanol and acetone (solvents) Antimony (III) ethoxide, co-dopant, (99.999% purity) Sigma Aldrich were used for sol preparations. The blue plus microscope glass slides were used as the substrates for sol coatings.

2.2. Methods

2.2.1. Preparation of SnO2:Ga Sol

$GaCl_3$-ultra dry, was dissolved in Acetyl acetone at room temperature. Table 1 illustrates the concentration composition values of SnO_2:Ga and Sb-co-doped SnO_2:Ga with the obtained thin films. At various concentration weights; 0.25 g, 0.5 g, 0.75 g and 1.0 g of Ga, the solution was refluxed at 70℃ using a reflux set-up for 2 hours to ensure effective homogenization. Hydrated $SnCl_4$ was then dissolved in ethanol in another beaker with the help of a magnetic stirrer at room temperature, cooled down and the solution added drop wise to the Ga dissolved solution. The sol was then aged in the dark room for 7 days [41] as in the flow chart in Figure 1 which illustrates the dissolving, refluxing and aging of the sol.

Table 1. The concentration composition values of SnO_2:Ga and Sb-co-doped SnO_2:Ga

Thin Film name	Concentration weight
Undoped (Sn)	1.2 ml
A (Sn + Ga	1.2 ml + 0.25 g
B (Sn + Ga)	1.2 ml + 0.5 g
C (Sn + Ga)	1.2 ml + 0.75 g
D (Sn + Ga)	1.2 ml + 1.0g
E (Sn + Ga + Sb	1.2 ml + 0.25 g + 0.5 ml
F (Sn + Ga + Sb)	1.2 ml + 0.5 g + 1.0 ml
G (Sn + Ga + Sb)	1.2 ml + 0.75 g + 1.5 ml
H (Sn + Ga + Sb)	1.2 ml + 1.0 g + 2.0 ml

2.2.2. Preparation of Sb-co-doped SnO_2:Ga Sol

After preparation of the gallium oxide sol, Antimony (III) Ethoxide was added in various concentrations of 0.5 ml, 1.0 ml, 1.5 ml and 2.0 ml (Table 1). The solution was then aged for 7 days to obtain the Sb-co-doped SnO_2:Ga coating sols as shown in flow chart (Figure 2) below;

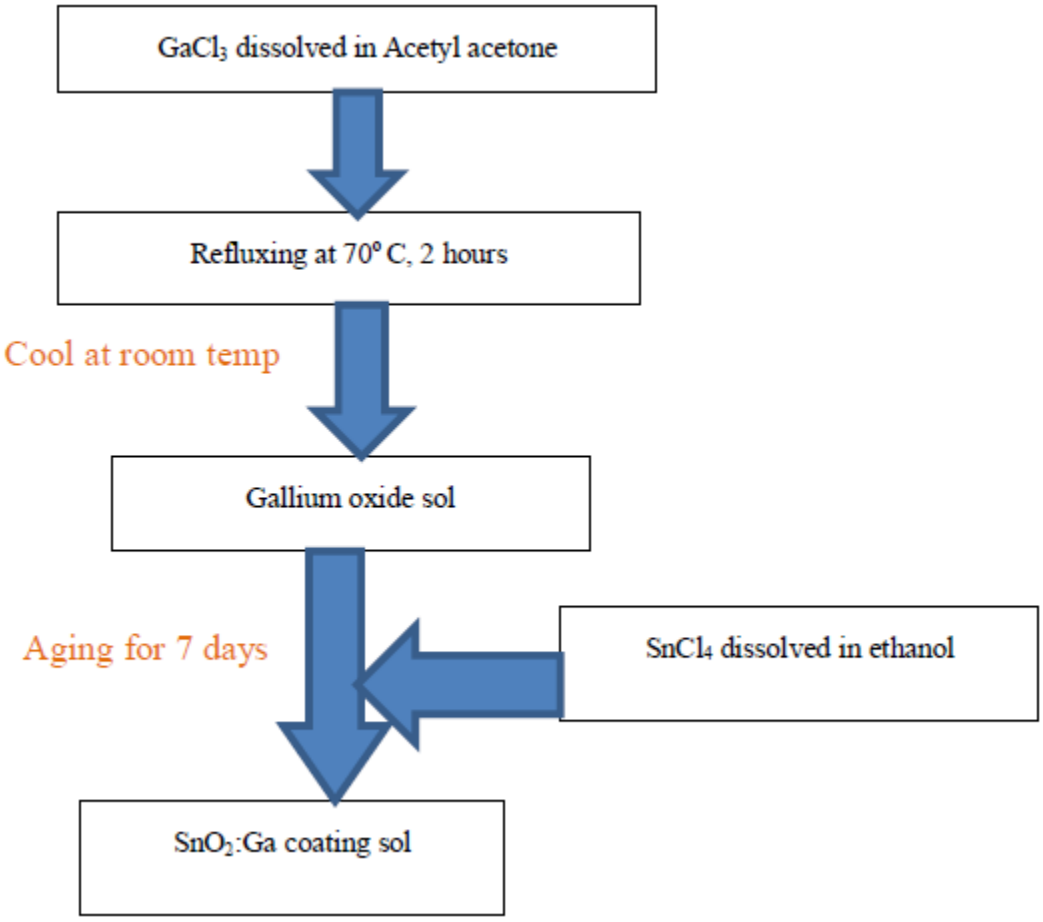

Figure 1. Flow chart of Preparation of SnO_2:Ga sol

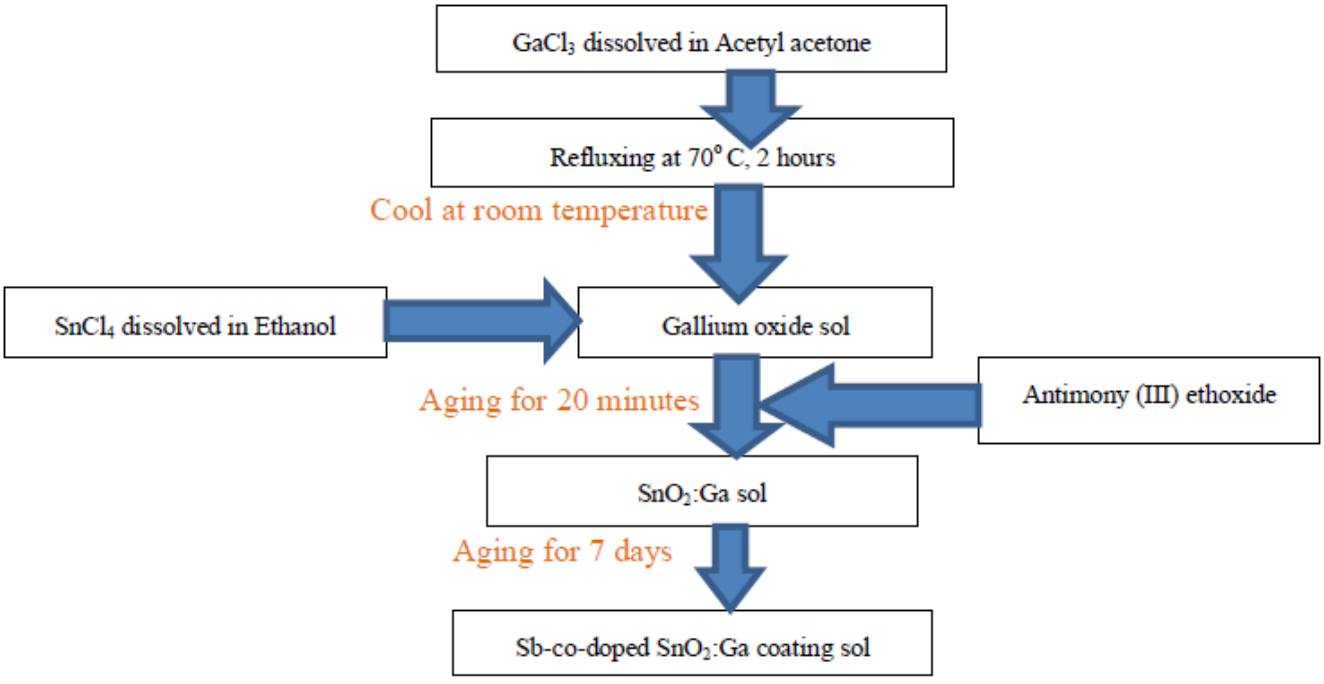

Figure 2. Flow chart of Preparation of Sb-co-doped SnO_2:Ga sol

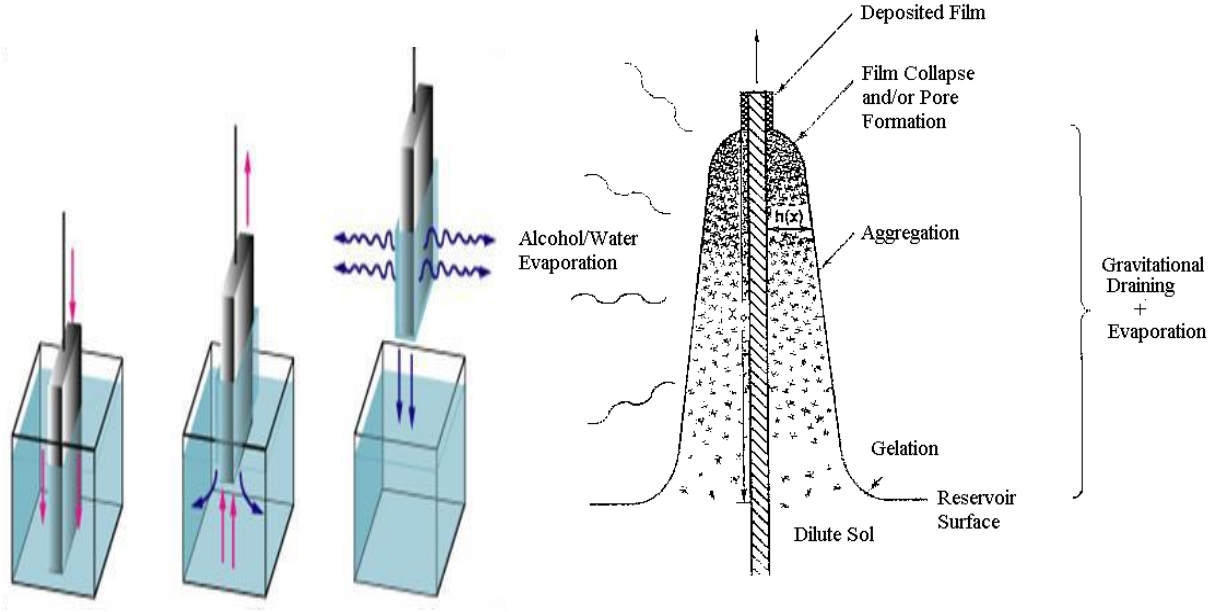

Figure 3. Schematic of the dip-coating [45] and withdrawal of substrate [46]

2.3. Preparation of Glass Substrates

Microscope glass substrates were used for sol coatings. The substrates were treated ultrasonically in ethanol and acetone and kept in a dessicator, ready for film deposition [43].

2.4. Film Deposition and Subsequent Treatment

Film deposition was carried out in air at room temperature by the dip-coating method (Figure 3) using the cleaned glass substrates. The substrates were left to dry horizontally at 50℃ in the oven to remove any organic residuals. The coating-drying procedure was repeated 3-times with an approximated withdrawal speed of 4 cm/min to obtain the desired film thickness [44]. The films were then annealed at 150℃ (optimal temperature) for 5 minutes and then cooled down at room temperature for crystal formation.

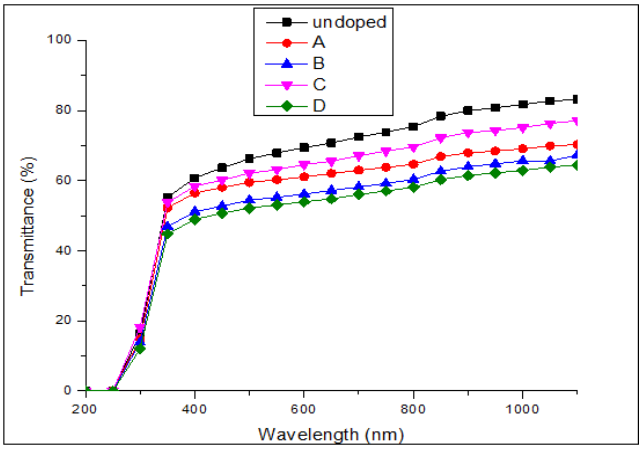

Figure 4. Transmission spectra for undoped (pure) SnO_2 and SnO_2:Ga thin Films (A-D)

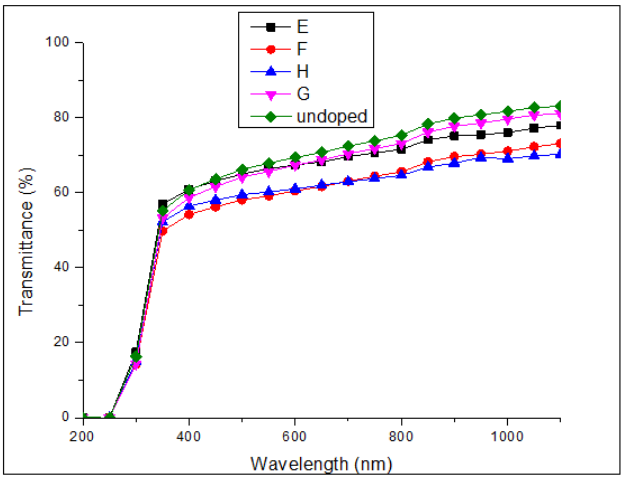

Figure 5. Transmission spectra for undoped (pure) and Sb-co-doped SnO_2:Ga thin films (E-H)

3. Results and Discussions

3.1. Optical Characterization

Optical transmission data were obtained using UV-Visible Scanning spectrophotometer (SHIMADZU 1800). The wavelength range was set at 200 nm-1100 nm. OriginPro 8.5 software was used to index the transmission data as shown in the spectra; Figure 4 and Figure 5.

Transmittance spectrum of the undoped (pure) SnO_2 thin film is transparent with an average transmittance ranging between (61.1-81.1) % at a wavelength range of between 400 nm to 900 nm respectively. The SnO_2:Ga films measures an average transmittance of about (50.4-72.6) % at a wavelength range of between 400 nm to 900 nm respectively. The Sb-co-doped SnO_2:Ga thin films indicates

a variation in the average transmittance of about 900 nm respectively. (53.6-78.1) % at a wavelength range of between 400 nm to

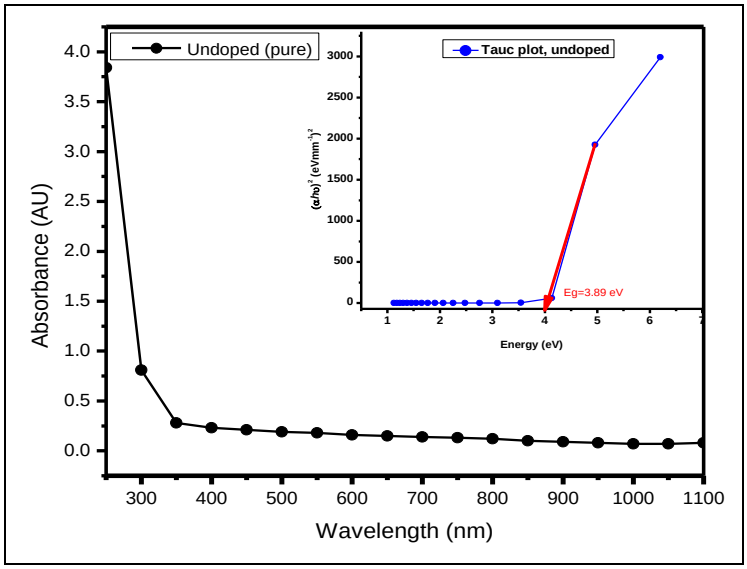

Figure 6. Tauc plots for the Undoped SnO_2

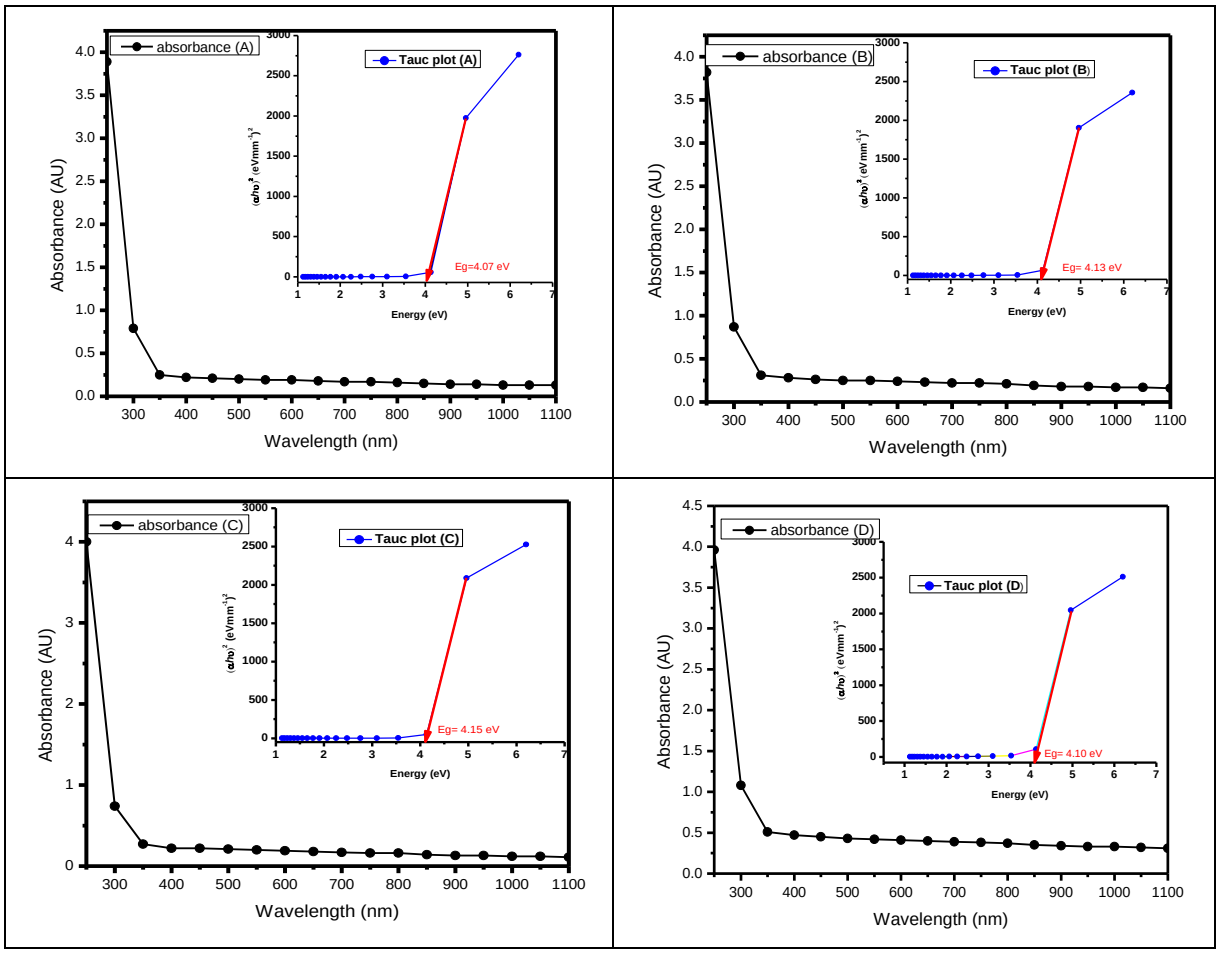

Figure 7. Tauc plots for SnO_2:Ga thin films (A)-(D)

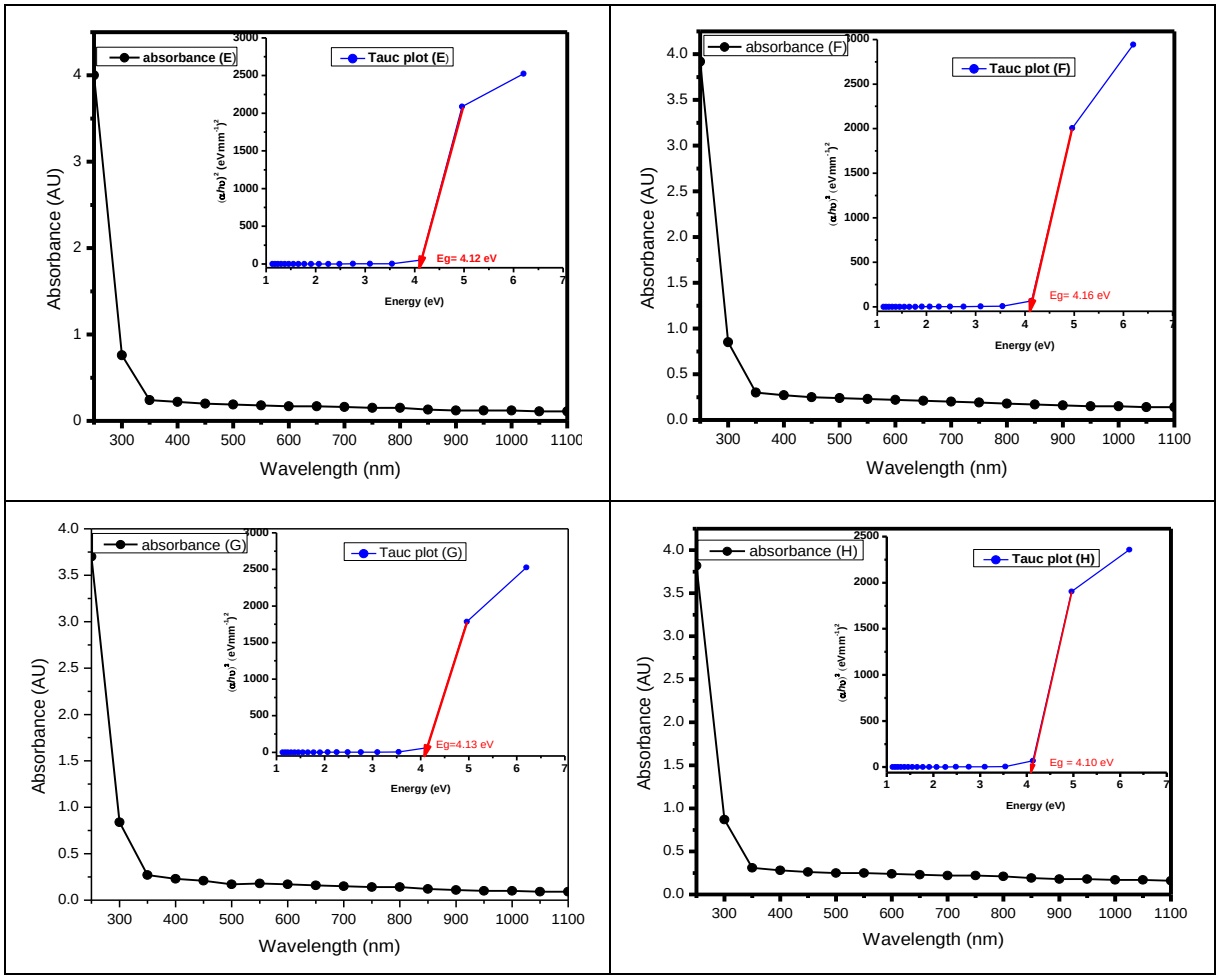

Figure 8. Tauc plots for Sb-co-doped SnO_2:Ga thin films **(E)-(H)**

A reduction in the average transmittance with increase in doping levels is observed for all the Ga doped and Sb-co-doped thin films. The Sb-co-doped SnO_2:Ga thin films measures a slightly higher average transmittance as compared to the Ga-doped SnO_2 thin films.

The Ga-doped starting sol also indicated a shift of the film colour from transparent to brown as the Ga concentration increased while the Sb-co-doped films indicated a shift of colour of the starting sol from transparent to light purple.

The 0.75 Ga-doped SnO_2 thin film C measure the highest transmittance as shown in figure 4 while the 0.75 Ga-doped with 1.5 ml Sb-co-doping thin film G, registered the highest transmittance as shown in Figure 5.

A similar effect of reduction in transmittance with doping is reported by Ramarajan *et al* [47] with spray-coated Sb-co-doped SnO_2 with Ba thin films and Peddavarapus *et al* [48] with sol-gel spin-coated Ga-doped films.

A reduction in average transmittance for all the doped thin films can be linked to the intrinsic nature of the film. This is due to dopant induced changes in the electronic structure of SnO_2 and also the change in the surface morphology which is usually manifested as change in its scattering.

The energy band gap is related to the optical absorption coefficient in a Tauc relation;

$$(\alpha hv)^m = B(hv - E_g)$$

Where B is a constant and E_g is the optical bandgap [49], [50].

The band gaps were computed from the extrapolation of $(\alpha hv)^2$ versus hv curves to the x-axis as shown in Figure 6, Figure 7 and Figure 8.

Undoped (pure) SnO_2 thin film measures a direct bandgap value of 3.89 eV. The SnO_2:Ga thin films measures band gap values of between 4.07 eV to 4.15 eV. Highest band gap value of 4.15 eV obtained for 0.75 g Ga-doped SnO_2, thin film C as shown in Figure 9. The Sb-co-doped SnO_2:Ga thin films measures band gap values of between 4.10 eV to 4.16 eV. Maximum band gap value of 4.16 eV registered for 1.0 ml Sb-co-doped 0.75 g SnO_2:Ga, thin film G as shown in Figure 10.

The bandgap value of the undoped thin film is 3.89 eV which corresponds to an absorption coefficient of 0.2073. The band gap values of the SnO_2:Ga thin films increases rapidly from 4.07 eV of 0.25 g Ga-doped thin film to 4.13 eV of 0.5 g Ga-doped thin film and 4.15 eV for 0.75g Ga-doped then decreases to 4.10 eV of 1.0 g Ga-doped thin film which measures the highest absorption coefficient.

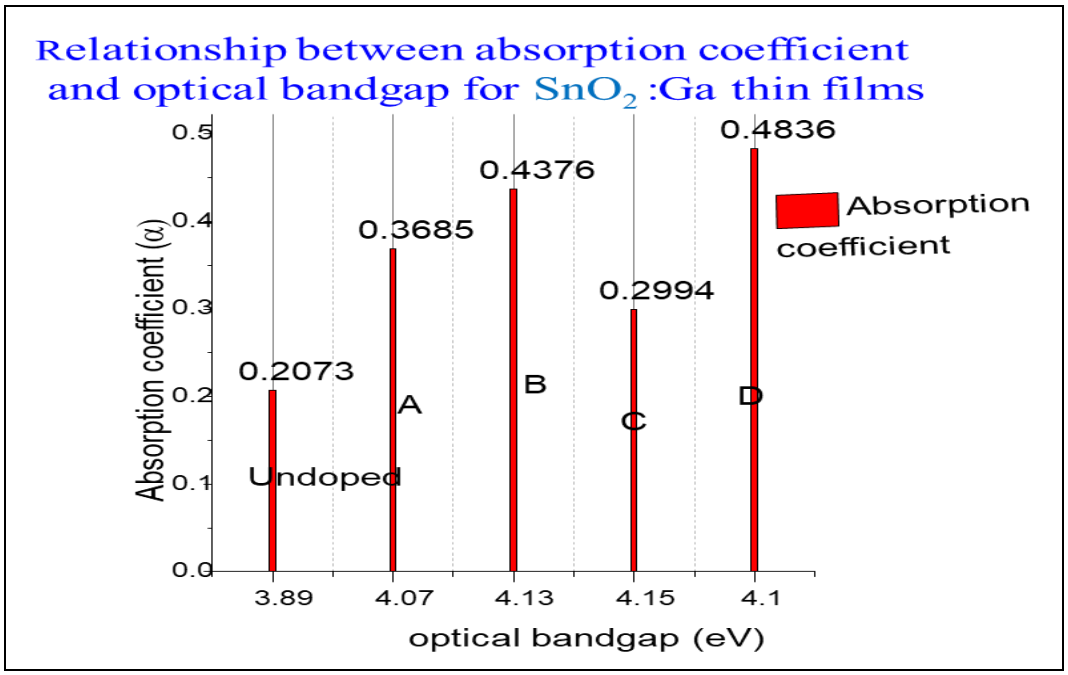

Figure 9. Relationship between absorption coefficient and optical band gap for SnO_2:Ga Thin films

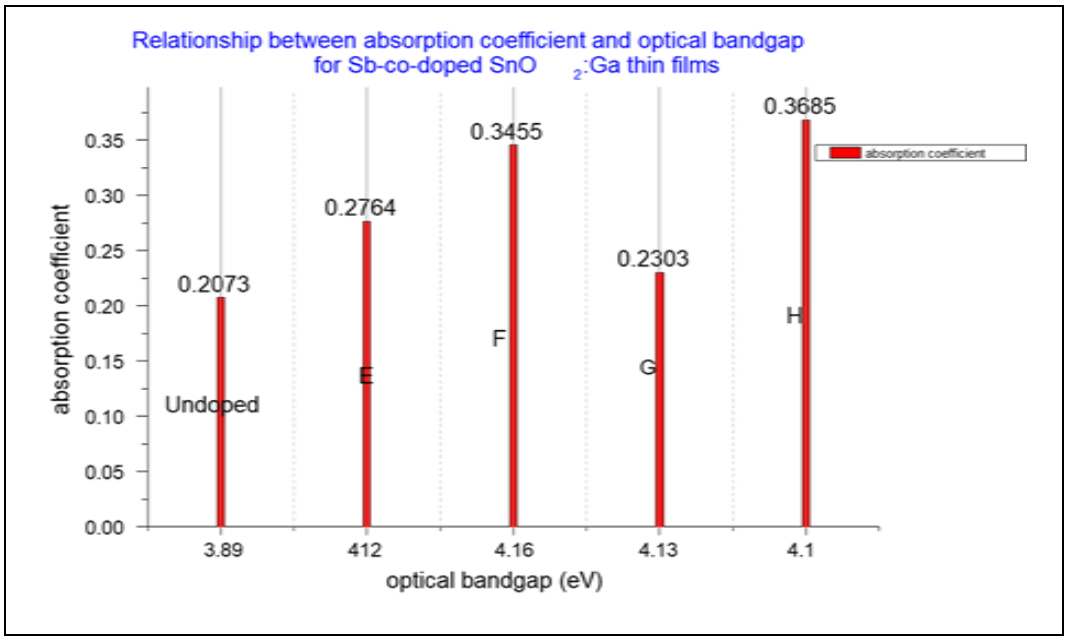

Figure 10. Relationship between absorption coefficient and optical band gap for Sb-co-doped SnO_2:Ga Thin films

A similar case is observed for the Sb-co-doped thin films. The bandgap values increase from 4.12 eV of 0.5 ml Sb-co-doped SnO_2:Ga film to 4.16 eV of 1.0 ml Sb-co-doped SnO_2:Ga film, decrease to 4.13 eV of 1.5 ml Sb-co-doped SnO_2:Ga film and then 4.10 eV of 2.0 ml of Sb-co-doped SnO_2:Ga film which measures the highest absorption coefficient.

A similar trend of bandgap widening and then narrowing for higher doping concentrations is reported by Benamar *et al* [51] for the ITO films prepared by spray pyrolysis, Thirumoorthi *et al* [52] with ITO thin films prepared by jet nebulizer spray pyrolysis technique, Vidhya *et al* [53] for gallium doped tin films prepared by spray pyrolysis technique and Nripasree *et al* [54] on the dopant induced and gap broadening in spray pyrolysed ZnCaO thin films.

The widening of the optical band gaps is directly related to dependance of the influence (coupling) of free carrier concentration as explained by Moss-Burstein effect on the fundamental absorption edge in the region of the near ultra-violet (UV) [55].

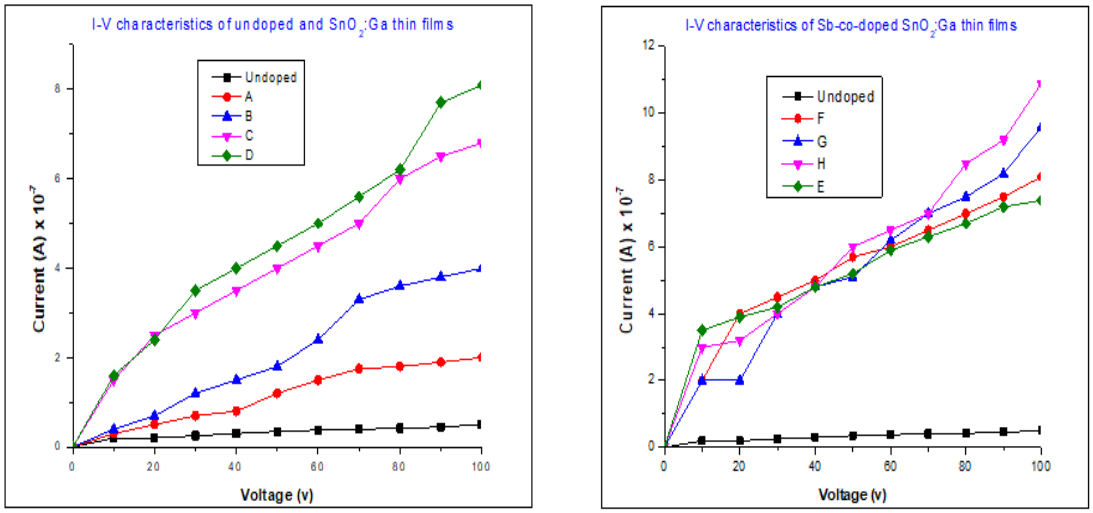

Figure 11. I-V characteristics of undoped (pure), SnO_2:Ga and Sb-co-doped SnO_2:Ga thin films

3.2. Electrical Characterization

Conductivity type of thin films was determined by a simple hot probe arrangement (Table 2). The tip of hot probe was heated to 120℃ of the cold probe with a separation distance of 15 mm placed on the surface of samples.

Table 2. Conductivity type of SnO_2:Ga and Sb-co-doped SnO_2:Ga thin films in various concentrations

Thin film	Charge type
Undoped (pure)	n-type conductive
A	p-type conductive
B	p-type conductive
C	p-type conductive
D	p-type conductive
E	p-type conductive
F	p-type conductive
G	n-type conductive
H	n-type conductive

The undoped SnO_2 thin film is n-type conductive. This is due to the creation of a native point-defect combination of oxygen vacancy plus the tin interstitial (V_o + Sn_i).

All the Ga-doped thin films are p-type conductive. A similar result discussed by Peddavarapu *et al* [48] with the influence doping of spin-coated Ga-doped SnO_2 thin films and Vidhya *et al* [53] with Ga-doped thin films prepared by spray pyrolysis method [53].

The Sb-co-doped thin films turned p-type at low co-doping levels of Sb. This is due to the fact that there are more of Ga^{3+} vacancies and Sb^{3+} state which for this case acts as acceptors hence creating more holes. Higher Sb-co-doped SnO_2:Ga thin films shifted to n-type conductive and can be directly related to an increase in carrier concentration attributed to high levels of Sb^{5+} in the thin film lattice and therefore creating shallow donor levels into the conduction band. It therefore enhances shift of the film to n-type conductive. The same trend of Sb behaviour while in the two states was observed by Esro *et al* [34] on the solution processed SnO_2:Sb.

However, Cao *et al* [56] reported a p-type conductivity of sputtered Sb-GaN films at higher doping levels of Sb.

Current-voltage response was utilized to determine the I-V characteristics of the thin films as shown in Figure 11 by a two point probe arrangement connected to a Keithley 6517B meter at room temperature with an applied input voltage from 10 to 100 [26].

Current values with corresponding voltage values linearly increase with the increase in Ga concentrations for the Ga-doped thin films. The Sb-co-doped thin films show improved I-V characteristics such that, the current values considerably increase with the increase in Sb-Ga concentrations as illustrated in Figure 10 above. This refers to a linear increase in conductivity of the films with the increase in Sb-Ga concentrations. Therefore, the resistivity of the prepared thin films is reduced.

This trend can directly be related to the ohmic behaviour of thin films.

A similar trend is reported by Ramarajan *et al* [47] with spin-coated Sb-co-doped $BaSnO_2$ thin films and Paul *et al* [57] with Lithium-Sb-co-doping prepared through spray pyrolysis method.

4. Conclusions

P-type Gallium doped tin oxide and Antimony co-doped Gallium-tin oxide thin films have been prepared on blue plus microscope glass substrates using the sol-gel dip-coating method. Optical and electrical properties of the prepared thin films were investigated. Transmittance spectrum of the undoped (pure) SnO_2 thin film was transparent with an average transmittance ranging between (61.1-81.1) % at a wavelength range of 400 nm to 900 nm respectively. The SnO_2:Ga films indicated an average transmittance of about

(50.4-72.6) % at a wavelength range of between 400 nm to 900 nm respectively. The Sb-co-doped SnO_2:Ga thin films measured a variation in the average transmittance of about (53.6-78.1) % at a wavelength range of between 400 nm to 900 nm respectively. A reduction in the average transmittance with increase in doping levels is observed for all the Ga doped and Sb-co-doped thin films. Undoped (pure) SnO_2 thin film measured a direct bandgap value of 3.89 eV. The SnO_2:Ga thin films indicated band gap values of between 4.07 eV to 4.15 eV. The Sb-co-doped SnO_2:Ga thin films with band gap values of between 4.10 eV to 4.16 eV. Highest band gap value of 4.15 eV was obtained for the SnO_2:Ga thin film and 4.16 eV for Sb-co-doped SnO_2:Ga thin film. Optical band gap widening and then narrowing was observed for all the Ga doped and Sb-co-doped thin films. The measured conductivity types of the thin films indicate an n-type charge for the undoped SnO_2 thin film. All the SnO_2:Ga thin films are p-type conductive. Low co-doped levels of Sb-co-doped SnO_2:Ga thin films are p-type conductive while for higher level co-doping of Sb a shift to n-type conductive is observed. The measured I-V characteristics of the thin films indicate a linear increase in current values with the corresponding voltage values as the concentrations of Ga and Sb increase indicating an increase in conductivity of the thin films as the Sb-Ga concentrations increase. This demonstrates a reduction in resistivity of all the prepared thin films.

In overall, both the undoped and doped thin films register a high average transmittance in the visible region with the n-type SnO2 at 81.1%, SnO2:Ga at 72.6% and Sb-co-doped SnO2:Ga at 78.1% good for use as transparent p-type contacts in thin film solar cells. The observed direct, wide band-gap values of the doped thin films with their respective absorption coefficients and band energies strongly depend on stoichiometric deviation and quantity of dopants available in the tin (host) lattice. The increase in voltage with current as the doping concentrations increases refers to a high electrical conductivity of the obtained thin film samples. Therefore, the improved optical and electrical properties of the obtained thin film samples validate their suitability in the solar cell applications.

REFERENCES

[1] Marc R.M. (2021). Transparent Ceramics: Materials, Processing, Properties and Applications; *Encyclopedia of Materials; Technical Ceramics and Glasses*, 1:399-423.

[2] Hadjadj A., and Gilliot M. (2023). Recent Advances in Functional Transparent Semiconductor Films and coatings; Coating, 13: 307.

[3] Pasquarelli R.M., Ginley D.S., and O'Hayre R. (2011). Solution Processing of transparent conductors: from flask to film; *Chemical Society Reviews*, 40: 5406.

[4] Tyagi M., Tomar M., and Gupta V. (2013). P-N Junction of NiO Thin Film for Photonic Devices. *IEEE Electron Device Letters*, 34(1): 81-83.

[5] Jaehoon, P. (2018). Solution-Processed Gallium-Tin-Based oxide Semi-conductors for Thin Film Transistors; *Materials*, 11(1): 3390.

[6] Mageto J., Mwamburi M., and Muramba W. (2012). The influence of Al doping on optical, electrical and structural properties of transparent and conducting SnO_2:Al thin films prepared by spray pyrolysis technique. *Elixir Chemical Physics*, 53(2012): 11922-11927.

[7] Vikash K.R., Ganesh B.M., and Angshuman N. (2016). Band Edge Energies and Excitonic Transition Probabiities of Colloidal CsPbX3 Perovskite Nanocrystals; *ACS Energy Letter*, 1-20.

[8] Benjamin A.D., John B., Jennilee B., Simon A., Robert G., and David O. (2017). Engineering Valenve Band Dispersion for High Mobility p-type Semiconductors; *Chemistry of Materials*, 29(6): 2402-2413.

[9] Hosono H., Hiramatsu H., Kamiya T., Tohei T., Ikenaga E., Mizoguchi T., Ikuhara Y., and Kobayashi K. (2010). Origins of hole doping and relevant optoelectronic properties of wide gap p-type semiconductor. *Journal of the American Chemical Society*, 132: 60-67.

[10] Kelvin Z., Kai X., Mark G., and Russel E. (2016). P-type transparent conducting oxides. *Journal of Physics Condensed Matter*, 28(38): 383002.

[11] Liu X., Zhang N., Tang B., Li M., Zhang Y., Yu G., and Gong H. (2018). Highly Stable New Organic–Inorganic Hybrid 3D Perovskite $CH_3NH_3PdI_3$ and 2D Perovskite $(CH_3NH_3)_3Pd_2I_7$: DFT Analysis, Synthesis, Structure, Transition Behavior and Physical Properties. *Journal of Physics and Chemistry Letters*, 9(19): 5862–5872.

[12] Sathyamoorthy R., Abhirami M., Gokul B., Gautam S., Chae K., and Asokan K. (2014). Fabrication of p-n junction diode using SnO/SnO_2 thin films and its device characteristics. *Electron Materials Letters*, 10: 743-747.

[13] Fumiyasu O., and Yu K. (2018). Design and exploration of semiconductors from first principles: *A review of recent advances;* Applied Physics Express, 11:6.

[14] Kanghoon Y., Yong Y., Miso L., Dongsun Y., Joohee L., Sung H., and Seungwu H.(2018). Computational Discovery of p-type transparent oxide semicondutors using hydrogen descriptor; *Computational Materia*ls, 17:4.

[15] Hosono H. (2007). Recent progress in transparent oxide semiconductors: Materials and device application; *Thin Solid Films*, 515:6000-6014.

[16] Robertson J., and Falabretti B. (2011). Electronic Structure of Transparent Conducting Oxides. *In book*: *Handbook of Transparent Conductor. Springer*, 2: 27-50.

[17] Batzill M., and Diebold U. (2005). The surface and materials science of tin oxide; *Progress in Surface Science*, 79: 47-154.

[18] Dolbec R., Khakani M.A., Serventi A.M., Trudeau R.G., and Saint R.G. (2002). Microstructure and physical properties of nanostructured tin oxide thin films grown by means of pulsed laser deposition; *Thin Solid F*ilms, 419:230-236.

[19] Galatsisi K., Cukrov L., Wlodarski P., McCormick K.,

Kalantar-zadeh E., Cominic G.(2003). P- and n-type Fe-doped SnO_2 gas sensors fabricated by the Mechano-chemical processing technique; *Sensors and Actuators B; Chemical*, 93:532-565.

[20] Teh J.J., Ting S.L., Leong K.C.., Li J., and Chen P. (2013). Gallium-Doped Tin Oxide Nano-Cuboids for Improved Dye Sensitized Solar Cell; *ACS Applied Materials and Interfaces*, 5(21): 11377-11382.

[21] Hsu C.L., Lu Y.C. (2012). Fabrication of a Transparent Ultraviolet Detector by using n-type Ga_2O_3 and p-type Ga-doped SnO_2 core-shell nanowires; *Journal of Nanoscale*, 4: 5710.

[22] Hong H.G., Song J.O., Na H., Kim K.K., Kim H., and Seong T.Y. (2007). Formation of Sb-Doped SnO_2 p-type Ohmic Contact from near-UV GaN-Based LEDs by a CIO Interlayer; Electrochemical and Solid State Letters, 10: H254.

[23] Presley R.E., Munsee C.L., Park C.-H., Hong D., Wager J.F., and Keszler D.A. (2004). Tin Oxide Transparent Thin-Film Transistors; *Journal of Physics D: Applied Physics*, 37; 2810-2813.

[24] Chien-Yie Tsay, Chun-Wei Wu, Chien-Ming Lei, Fan-Shiong Chen and Chung-Kwei Lin (2010). Microstructural and Optical properties of Ga-doped ZnO Semiconductor Thin Films prepared by Sol-gel Process; *Thin Solid Films*. 519: 1516-1520.

[25] Du J., and Ji Z.G. (2007). Effect of 1-Family Element Doping on Electronic Structures and Electrical Characteristics of SnO_2; *Acta Physica Sinica*, 56: 2388-2392.

[26] Singh A.K., Janotti A., Scheffler M., and Van de Walle C.G. (2008). Sources of Electrical Conductivity in SnO_2; *Physical Review Letters*, 101: 055502.

[27] Lee S.Y., and Park B.O. (2006). Structural, Electrical and Optical Characteristics of SnO_2:Sb thin Films by Ultrasonic Spray Pyrolysis; *Thin Solid Films*, 510:154-158.

[28] Lu Y., Wangn P., Zhang C.W., Feng X.Y., Jiang L., and Zhang G.L. (2011). First-principle on the Electronic and Optical properties of Mn-doped SnO_2; *Physica B: Condensed Matter*, 406: 3137-3141.

[29] Kumar V., Govind A., and Nagarajan R. (2011). Optical and Photocatalytic Properties of Heavily F-Doped SnO_2 Nanocrystals by a Novel Single-Source Precursor Approach; *Journal of Inorganic Chemical society*, 50:5637.

[30] Huang Y. Ji Z. and Chen C. (2007). Preparation and Characterization of p-type transparent conducting tin-gallium oxide films; *Applied Surface Science*, 253:4819-4822.

[31] Bagheri-Mohagheghi M.M., Shahtahamsebi N., Alinejad M.R., Youssefi A., and Shokoon-Saremi M. (2009). Fe-doped SnO_2 transparent semi-conducting thin films deposited by spray pyrolysis technique: Thermoelectric and P-type conductivity properties; *Solid State Sciences*, 11:233-239.

[32] Kong J. (2007). Synthesis and properties of pure and antimony-doped tin dioxide thin films fabricated by sol-gel technique on silicon wafer. *Materials Chemistry and Physics*, 114(2): 854-859.

[33] Jia T., Wang W., Long F., Fu Z., Wang H., and Zhang Q. (2009). Synthesis, Characterization, and Photocatalytic Activity of Zn-Doped SnO_2 Hierarchical Architectures Assembled by Nanocones; *Journal of Physical Chemical society*, 113:9071.

[34] Esro M., Georgakopoulos H., Lu H., Vourlias G., Krier A., Milne W.I., Gillin W.R., and Adamopoulos G. (2016). Solution Processed SnO_2:Sb Transparent Conductive Oxide as alternative to indium tin oxide for applications in organic light emitting diodes; *Journal of Material Chemical Society*, 4:3563-3570.

[35] Jago T., Eva G.B., Rocio O., Oihane H., Lucia M., and Javier B. (2021). Indium Tin Oxide Thin Films Deposition by Magnetron Sputtering at Room Temperature for the Manufacturing of Efficient Transparent Heaters; *Coatings*, 11(1):92.

[36] Jabbar H.K., Selma M.H., and Fadheela H.O. (2015). Preparation and Characterization of Tin Oxide Thin Films by Using spray pyrolysis Technique; *Engineering and Technology Journal*, 33(3B).

[37] Sapna D.P., Benjamin A.D., Sanjayan S., David O.S., Ivan P.P., and Claire J.C. (2018). Enhanced Electrical Properties of Antimony doped tin oxide thin films deposited via aerosol assisted chemical vapour deposition; *Journal of Materials Chemistry*.

[38] Jain P., Singh S., Siddqui A.M., and Srivastava A.K. (2012). Tin Oxide Thin Films Prepared by Thermal Evaporation Technique Under Different Vacuum Conditions; *Advanced Science, Engineering and Medicine*, 4:230-236(7).

[39] Jadhav H., Suryawanshi M.A., and Sinha S. (2017). Pulsed Laser Deposition of tin oxide thin films for emission studies; Applied Surface Science, 419:764-769.

[40] Aravin P.P., Mohanapriya V. Dana K., Jiri M. (2020). Progress in Sol-gel Technology for the Coatings of fabrics; *Material- Academic Open Access Publishing*, 13(8): 1838.

[41] Anna L., Alessandon C. and Maurizio F. (2017). Active Sol-Gel Materials, Fluorescence spectra, and Lifetimes; In: Klein L., Aparicio M., Jitianu A. (eds) *Handbook of Sol-Gel Science and Technology*, 1:1-43.

[42] Exarhos G. (2007). Discovery-based design of Transparent Conducting Oxide Films; *Materials Science Thin Solid Films*, 515(18): 7025-7052.

[43] Fredric S. (2018). Sol-Gel Technologies for Glass producers and users: Cleaning glass substrates. *Sprinker*, 3293: 19-34.

[44] Soraya H., Saeed R., and Suraya A. (2015). Grafting Carbon Nanotubes on Glass fiber by Dip-Coating Technique to enhance Tensile and Interfacial Shear Strength; *Journal of Nanomaterials*, 2015(7): 1497360.

[45] Abduladheem J., Supat C., Mohammed A., and Iman H. (2021). Nanomaterial by Sol-Gel Method: Synthesis and Application. *Advances in Materials Science and Engineering*, 21(2021): Article ID 5102014.

[46] Anna L., Alessandon C. and Maurizio F. (2017). Active Sol-Gel Materials, Fluorescence spectra, and Lifetimes. In: Klein L., Aparicio M., Jitianu A. (eds) *Handbook of Sol-Gel Science and Technology*, 1:1-43.

[47] Ramarajan R., Kovendhan M., Thangaraju K., Paul D., Ramesh R., Viswanathan E. (2020). Enhanced Optical transparency and Electrical conductivity of Ba and Sb-co-doped SnO_2 thin films; *Journal of Alloys and Compounds*, 153709.

[48] Peddavarapu S., Harish S.A., Ranjeth T., Srinvas G., Nagaiah K., Nanda N. (2021).Influence of Ga doping on Structural, Optical and Electrical properties of Transparent Conducting SnO_2 Thin Films; *Optik*, 226:165859.

[49] Goswami A. (1996). Thin Film Fundamental; *New Age International (P) Limited Publishers*- New Delhi.

[50] Xuan P., Feng J., Jin M., Ti Ning, Zhenguo S., Yongliang T., and Caina L. (2010). Structural and photoluminescence properties of SnO_2:Ga films deposited on Al_2O_3(0001) by MOCVD; *Journal of Luminescence*, 130:1189-1193.

[51] Benamar E., Rami M., Messaoudi C., Sayah D., and Ennaoui A. (1999). Structural, Optical and Electrical properties of Indium tin oxide thin films prepared by spray pyrolysis*; Solar Energy Materials and Solar Cells*, 56:125-139.

[52] Thirumoorthi M., and Thomas J. (2016). Structural, Optical and Electrical properties of Indium tin oxide ultra-thin films prepared by jet nebulizer pray pyrolysis technique; *Journal of Asian Ceramic Societies*, 4:124-132.

[53] Vidhya S.N, Balasundaram O.N., and Chandramohan M. (2016). Structural and Optical Investigations of gallium doped tin films prepared by spray pyrolysis; *Journal of Saudi Chemical Society*, 20: 703-710.

[54] Nripasree N., Deepak NK. (2018). Ga Dopant Induced Band gap Broadening Conductivity enhancement in spray pyrolysed $Zn_{0.85}Ca_{0.15}O$ thin films; Materials Research, 21(6).

[55] Burstein E. (1954). Anamolous Optical Absorption limit in InSb; *Physical Review*, Crystal Branch, Metallurgy Division, Naval Research Laboratory, Washngton, D, 93: 632-633.

[56] Cao P., Thi A., Dong K., Wen K., Thach N. (2020). Reactively Sputtered Sb-GaN Films and its Hetero-Junction Diode; *The Exploration of the n-to-p Transition*, 10(3):210.

[57] Paul D., Devarajan U., Jean F., Ramarajam M., Korendhan M., Nandarapu P., Reddivari M., Venkatenswan C. (2021). Lithium-antimony co-doping induced Morphology transition in spray deposited SnO_2 thin films; *Surfaces and Interfaces*, 23: 100918.